International Journal of Civil Engineering and Technology (IJCIET)
Volume 10, Issue 06, June 2019, pp. 35-42, Article ID: IJCIET_10_06_004
Available online at http://www.iaeme.com/ijciet/issues.asp?JType=IJCIET&VType=10&IType=6
ISSN Print: 0976-6308 and ISSN Online: 0976-6316

MEASUREMENT OF LOCAL MECHANICAL CHARACTERISTICS OF MARBLE BY BROADBAND ULTRASONIC STRUCTUROSCOPY

A.N., Kravcov, I.A., Shibaev
Czech Technical University in Prague, Faculty of Civil Engineering,
Department of Technologies, Thákurova 7, Prague, 166 29, Czech Republic

ABSTRACT

The internal structure of marble is investigated. A precise measurement of the speeds of longitudinal and moving waves in marble samples. The internal structure of samples is visualised and localised microcracks. The geometric sizes of the microcracks are determined. Using the obtained velocity values, the Young's modulus and porosity were calculated. According to the research and calculations, the effectiveness of using marble as a facing stone in urban and industrial areas was made.

Key words: Exterior cladding material, marble, civil construction, laser ultrasonic structuroscopy, non-destructive testing.

Cite this Article: A.N., Kravcov, I.A., Shibaev, Measurement of Local Mechanical Characteristics of Marble By Broadband Ultrasonic Structuroscopy, *International Journal of Civil Engineering and Technology* 10(6), 2019, pp. 35-42.
http://www.iaeme.com/IJCIET/issues.asp?JType=IJCIET&VType=10&IType=6

1. INTRODUCTION

Recently, natural stone exterior wall cladding has been increasingly used in civil and religious construction and in the restoration of historic architectural buildings [1, 2]. Stone cladding of historic buildings in European cities are in need of restoration because of its unsatisfactory condition. Some stone elements of facades are delaminated; stonework is badly damaged by weathering processes causing parts of stonework to crack, crumble, stain, etc. Also, historic building exteriors are deteriorated due to increase of atmospheric pollution and vibrational loading and also due to changes in soil hydro-dynamic properties, which may cause the subsidence and consequent deformation of the buildings, etc. [3, 4].

Marble, which has been widely used to manufacture architectural elements and sculptural masterpieces for centuries, is very sensitive to temperature changes because of the anisotropic properties of calcite crystallites, which causes inelastic deformation and microcracks [5, 6]. The thermal expansion combined with sulfation may cause serious microstructural damage and eventually granular disintegration of marble [7].

As a result, the strength and performance characteristics of marble gradually deteriorate, which means that the cladding is likely to fail in the end, not to speak of the fact that its aesthetic appearance is negatively affected. For this reason, outstanding architecture buildings look like if they are perfectly mediocre buildings.

The most serious consequences of cladding deterioration are usually due to a wrong choice of cladding material. If a natural stone material is insufficiently resistant to cold and acid or there was breach of mining regulations and standards during its extraction, defects in the cladding become visible within a short period.

Today, various monitoring methods are used to examine the structure of facing stones, including optical and electron microscopy [8], X-ray tomography [9,10], ultrasonic methods [11,12], etc. Ultrasonic testing is most commonly used in assessing building materials [11,12] and cultural heritage stone artworks [13,14]. Ultrasonic methods are used for the detection of surface and internal defects, measurement of the thickness of layers in multilayer materials, and evaluation of volumetric mechanical properties based on longitudinal and shear wave velocities. These applications usually use the frequen-cy range from 50 to 500 kHz, which makes it possible to examine samples tens of centimeters thick with a spatial resolution of up to 1cm. The use of frequencies above 1 MHz is limited because of their strong attenuation in marble and other facing materials [15, 16, 17].

Spatial resolution can be higher provided that the amplitude of the ultrasonic probe pulse is several orders of magnitude greater and the frequency is a few tens of MHz This can be attained by means of laser-based excitation of acoustic pulses and reception of ultrasonic energy by a broadband piezoelectric transducer [18-20]. The use of a Q-switched laser generating pulses with duration of around 10 ns and energy of several mJ, which in turn generates ultrasonic pulses with less than 70 ns duration and pressure amplitude of up to 1 MPa, allows an excellent spatial resolution of about 50 μm to be achieved. Therefore, it is possible to detect a variety of microstructures and heterogeneities and assess their dimensions (size of crystals, porosity, and degree of weathering) in pulse-echo mode [19,20].

This paper describes a study of local physical and mechanical characteristics of marble samples by laser ultrasonic spectroscopy able to visualize the internal structure of materials.

2. MATERIALS AND METHODS

2.1. Optoacoustic Equipment and Measuring Technique

The generation of ultrashort high-power ultrasonic pulses with a strictly controlled form occurs in an optoacoustic cell. Fig. 1 shows a schematic diagram of this cell for diagnostics of materials at one-side access. A 10-ns 0.1 mJ pulse generated by a Nd: YAG laser is transmitted to the front side of a special optoacoustic generator (OAG) via an optic fiber cable, an optical beam forming system, and a transparent prism. The OAG is a plane-parallel plate made of ad hoc plastic absorbing light. The trans-parent prism is in acoustic contact with the OAG, being at the same time a sound conducting channel of a broadband piezoelectric transducer made of polyvinylidene fluoride (PVDF) film. One-side access and acoustic contact are ensured by pressing the OAG plane to the front side of the object with a thin layer of contact fluid between (e.g. distilled water).

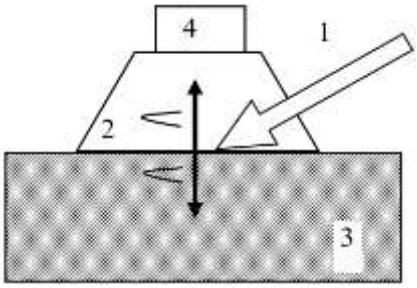

Figure 1 Schematic diagram of optoacoustic generator: 1 - laser pulse, 2 - transparent prism a plane-parallel plate made of ad hoc plastic absorbing light in the end, 3 - sample, 4 - broadband piezoelectric transducer

Laser pulse absorption by the near-surface layer of the OAG and subsequent thermal expansion produce an ultrasonic pressure pulse with known temporal shape and amplitude. The pulse wave propagates through the prism to be recorded by the piezoelectric sensor (direct wave) and towards the sample where it is partially reflected at the OAG-sample interface due to difference in acoustic impedance; this reflection is recorded by the piezoelectric sensor with the time delay equal to the double travel time in the OAG. The remainder of the pulse energy enters the sample and is scattered by its heterogeneities and reflected from the back side of the sample. In the case of sufficiently strong scattering (which is indicative of high degree of heterogeneity), the reflection from the back-side may be not be observed [21].

All scattered and reflected signals are recorded by the piezoelectric transducer and processed by a processing system. Fig. 2 shows a resulting acoustic track (so-called A-scan). The surface of the sample is scanned with a 1 mm step (Fig. 3); the resulting A-scans are "sewn together" to produce a 2D image of the internal structure of the sample. Provided that the reflection from the back side of the sample is distinctly recorded (no defects and low porosity), the phase velocity of longitudinal ultrasonic waves can be evaluated:

$$V_l = 2H/\Delta T \qquad (1)$$

where $\Delta T = T_1 - T_0$ is the difference between the arrival times of the minimum of the reflection from the back side and the maximum of the reflection from the OAG-sample interface; H is the thickness of the sample. The depth of a major defect Z_d can be determined from the arrival time of the reflection from it:

$$Z_d = V_l \Delta T_d / 2 \qquad (2)$$

where $\Delta T_d = T_d - T_0$ is the difference between the arrival times of the reflection from the defect and the reflection from the OAG-sample interface (in Fig 1). Thus, in the case of indirect reading, laser ultrasonic structuroscopy is similar to traditional ultrasonic systems operating in echo-pulse mode.

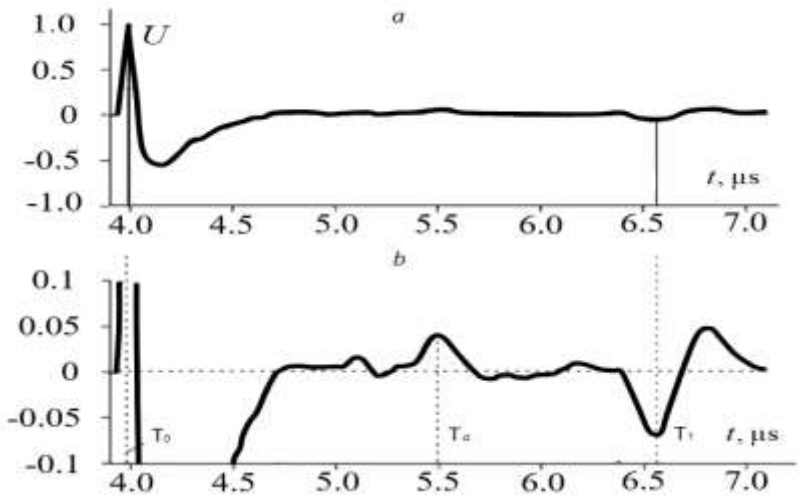

Figure 2 A resulting acoustic track: a - full signal, b - a signal fragment with a tenfold increase in the ordinate axis.

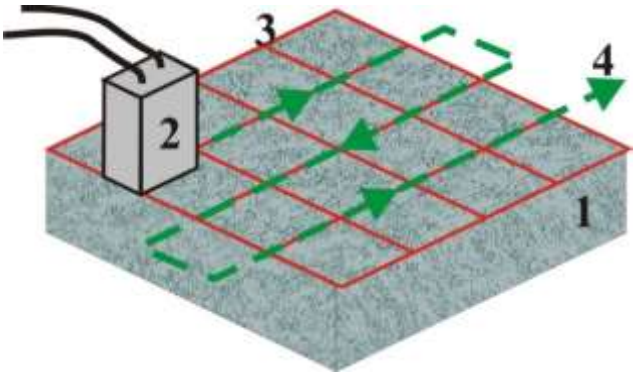

Figure 3 Scheme of optoacoustic scanning: 1-sample; 2-OAG; 3-scan surface; 4-path of OAG movement

Note that an S-wave pulse is recorded in the interval between the first and second reflections of P-waves from the back side; the time delay of the S-wave arrival can be used to calculate its velocity. In the course of scanning, local velocities are determined. Using the velocities dependent on density and local moduli of elasticity; modules are calculated as follows:

$$E = \rho C_t^2 \left[3 - \frac{1}{x^2 - 1} \right], \tag{3}$$

$$\nu = \frac{x^2 - 2}{2(x^2 - 1)}, \tag{4}$$

$$G = \rho C_t^2, \tag{5}$$

where: E is Young's modulus, G is shear modulus, ν is Poisson's ratio, ρ is the calculated density of the sample, C_t is the measured value of shear acoustic wave velocity in the sample,

m/s; C_l is the measured value of longitudinal acoustic wave velocity in the sample, m/s; $x = C_l / C_t$ is the ratio of the longitudinal and shear wave velocities.

Based on the above-described, it is possible to map ultrasonic wave velocities and elastic modules.

3. SAMPLES

The marble samples considered in this paper, were received from Koelga deposit, the largest in Russia and one of the largest in the world. Koelga marble plates are widely used for facing columns and interiors walls of buildings and structures, for decoration of the vestibules of metro stations, etc. The viscosity of marble allows it to be used for decorative purposes. The samples studied are rectangular parallelepipeds with the characteristic dimensions 40 mm, 35 mm, and 3-8 mm (Fig. 4). Images of microsections (Figs. 5a and 5b) produced by a Phenom ProX electron microscope exhibit clearly visible intergranular boundaries and pores (dark color); the size of grains ranges from 50 μm to 400 μm; most grains characteristically have a size of 200 μm, porosity is rather low. The physical and mechanical properties of the samples are as follows: the average density is 2700 kg/m3, the ultimate compression strength varies from 65 to 100 MPa, water absorption is 0.16%.

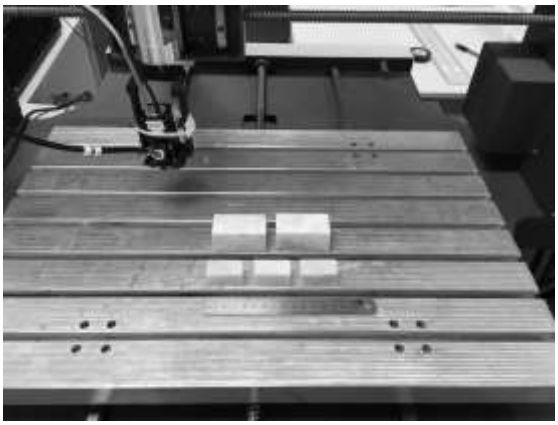

Figure 4 Photos of samples

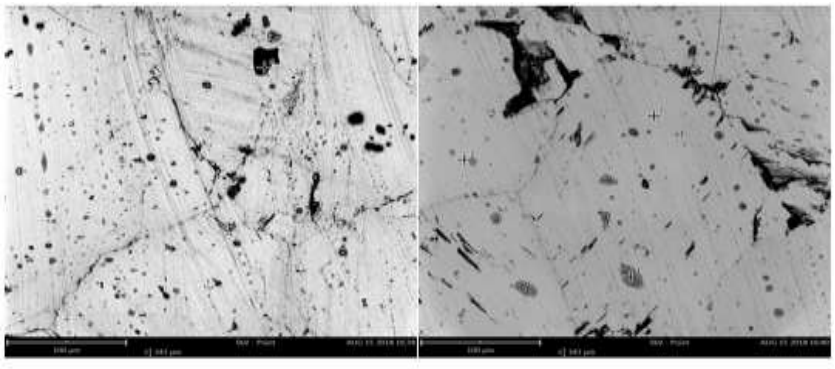

a b

Figure 5 Phenom ProX3 SEM images of polished sections

4. RESULTS

The samples were scanned with a step of 300 μm. Based on 2D images of their internal structure, the samples can be divided into two groups. The first group includes samples with

cracks 500 μm or more in size. Fig. 6, a shows the internal structure of one of these samples. Here, there is a crack 2,2 mm long at a depth of 3 mm. The second group includes samples with microcracks and pores smaller than 500 μm in size. The internal structure of such a sample is shown in Fig. 6, b. The initial structure of the sample is fairly homogeneous (acoustical impedances at all points slightly differ from the average value), only some scan planes have small regions with higher acoustic impedance, which is accounted for by the presence of "harder" minerals (i.e. the lighter-shaded region several millimeters in size in Fig. 6, b).

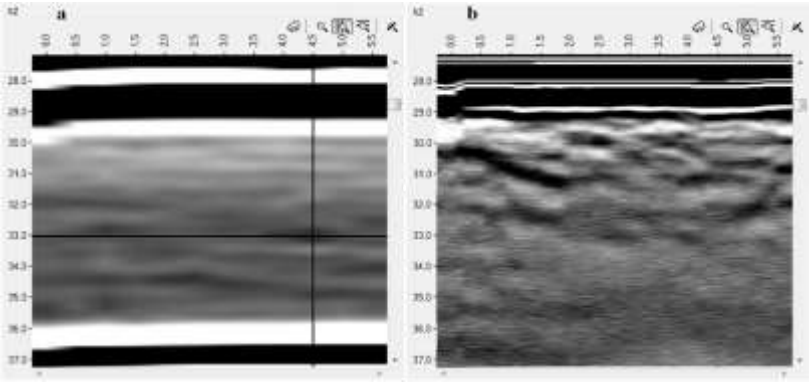

Figure 6 Visualization of the internal structure of marble samples: with a crack 2,2 mm long (a) and with-out defects (b)

Defect-free marble samples were selected to be further examined. Fig. 7-8 show maps of elastic wave velocities, elastic moduli, and porosity for one of the samples. Clearly (Figs. 7 and 8), this marble sample is quite homogeneous, longitudinal and shear wave velocities vary from 6360 to 6480 m/s and from 2220 to 2300 m/s, respectively; Young's modulus and Poisson's ratio vary from 38.0 to 40.5 GPa and from 0.428 to 0.433, respectively. Porosity is low, no more than 0.7%.

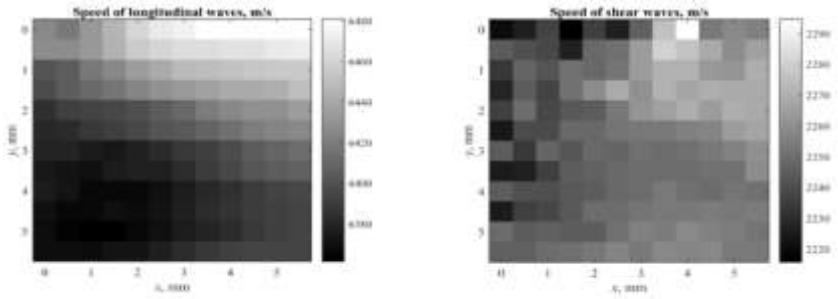

Figure 7 Maps of elastic longitudinal (a) and shear (b) wave velocities

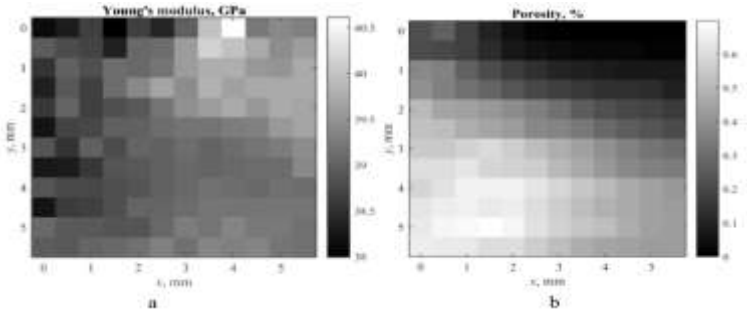

Figure 8 Young's modulus (a) and porosity (b) maps of marble sample

5. CONCLUSIONS

It is found that the use of laser ultrasonic structuroscopy opens new opportunities to evaluate the quality of facing stones and the integrity of stone artworks. Precise measurement of elastic wave velocities with an error of 0.5% makes it possible not only to visualize the internal structure of samples and evaluate the degree of their heterogeneity, but also to measure the local moduli of elasticity and porosity.

REFERENCES

[1] S.B. Sadineni, S. Madala, R.F. Boehm, "Passive building energy savings: A review of building envelope components," *Renewable and Sustainable Energy Reviews*, vol. 15, issue 8, pp. 3617-3631, October 2011.

[2] A.S. Guimaraes, J.M.P.Q. Delgado, V.P. de Freitas, "Treatment of rising damp in historic buildings: Experimental campaign of wall base ventilation and interface effect analysis," *Journal of Cultural Heritage*, vol. 20, pp. 733-773, July 2016.

[3] E. Cardarelli, G. de Donno, C. Scatigno, I. Oliveti, M. Preite Martinez, N. Prieto-Taboada, "Geophysical and geochemical techniques to assess the origin of rising damp of a Roman building (Ostia Antica archaeological site)," *Microchemical Journal*, vol.129, pp. 49-57, November 2016.

[4] S. Madureira, I. Flores-Colen, J. de Brito, C. Pereira, "Maintenance planning of facades in current buildings," *Construction and Building Materials*, vol. 14, pp. 790-802, November 2017.

[5] A. Murru, D. M. Freire-Lista, R. Fort, M. J. Varas-Muriel, P. Meloni, "Evaluation of post-thermal shock effects in Carrara marble and Santa Caterina di Pittinuri lime-stone," *Construction and Building Materials*, vol. 186, pp. 1200-1211, October 2018.

[6] V. Becattinia, T. Motmansa, A. Zapponeb, C. Madonnab, A. Haselbachera, A. Steinfelda, "Experimental investigation of the thermal and mechanical stability of rocks for high-temperature thermal-energy storage," *Applied Energy*, vol. 203, pp. 373-389, October 2017.

[7] Nabil.A. Abd el-Tawab, "Degradation and conservation of marble in the greek roman hadrianic baths in leptis magna, libya," *International Journal of Conservation Science*, vol. 3, issue 3, pp. 163-178, July-September 2012.

[8] N.N. Potravkin, E.B. Cherepetskaya, I.A. Perezhogin, V.A. Makarov, "Ultrashort elliptically polarized laser pulse interaction with helical photonic metamaterial," *Optical Materials Express*, vol. 4, issue 10, pp. 2090-2101, October 2014.

[9] A. Kravcov, P. Svoboda, A. Konvalinka, E.B. Cherepetskaya, I.E. Sas, N.A. Morozov, J. Zatloukal, "Evaluation of crack formation in concrete and basalt specimens under cyclic uniaxial load using acous-tic emission and computed X-Ray Tomography" *KEM*, vol. 722 pp. 247-253, October 2016.

[10] I.A. Shibaev, E.B. Cherepetskaya, A.S. Bychkov, V.P. Zarubin, P.N. Ivanov, "Evaluation of the internal structure of dolerite specimens using X-ray and laser ultrasonic tomography," *International Journal of Civil Engineering and Technology*, vol. 9, issue 9, pp. 84-94, December 2018.

[11] . X. Li, Y. Song, F. Liu, H. Hu, P. Ni, "Evaluation of mean grain size using the multiscale ultrasonic attenuation coefficient," *NDT & E International*, vol. 72, pp. 25-32, October 2015.

[12] S. Fais, G. Casula, "Application of acoustic techniques in the evaluation of terogeneous building materials," *NDT & E International*, vol. 43, issue 2, pp. 62-69, June 2010.

[13] El. Zendri, L. Falchi, Fr. C. Izzo, Z. M. Morabito, G. Driussi, "A review of common NDTs in the monitoring and preservation of historical architectural surfaces," *International Journal of Architectural Heritage*, vol. 11, issue 7, pp. 987-1004, May 2017.

[14] G. Luchin, L.F. Ramos, M. D'Amato, "Sonic Tomography for Masonry Walls Characterization," *Inter-national Journal of Architectural Heritage*, December 2018. [doi.org/10.1080/15583058.2018.1554723]

[15] Stoller, J., E. Zezulova. 2017. „Use of ultrasound-The ultrasonic pulse velocity method for the diagnosis of protective structures after the load of TNT explosion", pp. 230-235 in ICMT 2017 - 6th International Conference on Military Technologies, http://dx.doi.org/10.1109/MILTECHS.2017.7988761.

[16] S. N. Iliopoulos, L. de Smet, D. G. Aggelis, "Investigating ultrasonic wave dispersion and attenuation in fresh cementitious materials: A combined numerical, analytical, and experimental approach," *NDT & E International*, vol. 100, pp.115-120, December 2018.

[17] S.N. Iliopoulos, L. de Smet, D.G. Aggelis "Investigating ultrasonic wave dispersion and attenuation in fresh cementitious materials: A combined numerical, analytical, and experimental approach," *NDT & E International*, vol. 100, pp. 115-123, December 2018.

[18] D.S. Uryupina, A.S. Bychkov, D.V. Pushkarev, E.V. Mitina, A.B. Savelev, O.G. Kosareva, N.A. Panov, A.A. Karabutov, E.B. Cherepetskaya, "Laser optoacoustic diagnostics of femtosecond filaments in air using wideband piezoelectric transducers," *Laser Physics Letters*, vol. 13, issue 9, pp.095401, September 2016.

[19] D. Ciofini, A.A. Mencaglia, S. Siano, "A photoacoustic pulse-echo probe for monitoring surface stone mechanical properties: Validation tests in consolidation of Carrara marble," *Construction and Building Materials*, vol. 187, pp. 610-619, October 2018.

[20] A. Kravcov, I.A. Shibaev, D.I. Blokhin, A.S. Bychkov, E.B. Cherepetskaya, M.M. Krapivnoi, V.P. Zarubin, "Examination of structural members of aerial vehicles by laser ultrasonic structuroscopy," *International Journal of Civil Engineering and Technology*, vol. 9, issue 11, pp. 2258-2265, November 2018.

[21] A.S. Bychkov, E.B. Cherepetskaya, A. Konvalinka, A.A. Karabutov, A. Kravcov, V.A. Makarov, E.A. Mironova, N.A. Morozov, "Study of the internal structure of isotropic pyrolytic graphite by broadband ultrasonic spectroscopy," *Lecture Notes in Mechanical Engineering*, vol. 11, part F, pp. 1-7, 2017.